Two-fluid sub-grid-scale viscosity in nonlinear simulation of ballooning modes in a heliotron device

H. Miura[1], F. Hamba[2] and A. Ito[1]

[1]National Institute for Fusion Science (NIFS), Toki, Japan
[2]Institute of Industrial Science (IIS), the University of Tokyo, Tokyo, Japan

Corresponding Author: miura.hideaki@nifs.ac.jp

Abstract:
A Large Eddy Simulation (LES) approach of full-3D extended magnetohydrodynamic (MHD) equations is introduced to enable studying nonlinear growth of ballooning modes in a heliotron-type device over a wide range of parameter space as easily as possible. A model to substitute influences of the scales smaller than the grid size, Sub-Grid-Scale (SGS), on the scales larger than the computational Grid Scale (GS) is developed. An LES of two-fluid MHD equations with the SGS models successfully reproduces growth of the ballooning modes and nonlinear saturation, showing usefulness of the LES approach to study the instability in a heliotron device with a small computational cost.

1 Introduction

Physics of mild saturation of ballooning and interchange modes has been studied as one of the essential subjects for a heliotron device[1, 2, 3, 4]. While linear stability analysis predicts emergence of ballooning/interchange instability for the magnetic axis position $R_{ax} = 3.6m$ of the Large Helical Device (LHD), a high β-value of about 5.1% has been achieved in LHD experiments. Because MHD activity is observed during discharges, it has been considered that linearly unstable modes grow but the growth is saturated mildly. Since understanding physics of mild saturation has been an important issue in order to achieve a higher β, some numerical works have been devoted to clarify the mechanics of the mild saturation. Though it has been shown by a 3D MHD simulation that the instabilities can be saturated mildly when a large viscosity μ is adopted[3], it is difficult to justify the large value. Pressure flattening, fluid compressibility, parallel heat conductivity and parallel flow generations can also help the mild saturation in full 3D simulations[1, 3, 5]. However, it has been also shown by full-3D compressible MHD simulations by the use of the MHD In the Non-Orthogonal System (MINOS) code in Ref.[1] that the pressure can be collapsed even with the help of these candidates. Numerical simulations by the use of another full-3D numerical code, MIPS[6], have also shown that the pressure can be

collapsed when unstable ballooning modes grow.[2] It is now argued that micro-physics such as two-fluid effects (such as diamagnetic flow) and the gyro-viscosity and flow shear effects can suppress the instability.

A two-fluid 3D numerical simulation is an important tool to clarify the mechanism of the mild saturation. Since we pay much attention on nonlinear dynamics together with relatively large amplitude of magnetic and pressure fluctuations, we retain both two-fluid (Hall) and gyro-viscous terms explicitly into the simulations. A difficulty in such a strongly nonlinear simulation is that scales which are not resolved in a simulation can be important through nonlinear couplings, while very fine simulations suffer from existence of whistler waves and small-scale activities such as secondary Kelvin-Helmholtz-like instability as has been reported in Ref.[7]. Since the artificial truncation of the small scales often contaminates and ruins nonlinear dynamics of GS modes[4, 7], it is required to compensate the influences of the unresolved scales by a SGS model. In this paper we focus on influences of the unresolved scales in a two-fluid simulation and develop a SGS model. Recently we have shown that a SGS model in Ref.[8] can be applicable to two-fluid (Hall) MHD turbulence[9], based on our earlier numerical simulations[4]. Here the SGS model is applied for ballooning simulations.

2 Extended MHD equations in the grid scale and SGS models

In the MINOS code, the 3D extended MHD equations

$$\frac{\partial \rho}{\partial t} = -\frac{\partial (\rho u_i)}{\partial x_j}, \tag{1}$$

$$\frac{\partial (\rho u_i)}{\partial t} = -\frac{\partial}{\partial x_j}(\rho u_i u_j + p\delta_{ij}) + \epsilon_{ijk} J_j b_k + \frac{\partial \Pi_{ij}}{\partial x_j}, \tag{2}$$

$$\frac{\partial p}{\partial t} = -\frac{\partial}{\partial x_k}(p u_k) + (\Gamma - 1)\left(-p\frac{\partial u_j}{\partial x_j} + \eta J_k J_k + u_i \frac{\partial \Pi_{ij}}{\partial x_j} - \frac{\partial q_j}{\partial x_j}\right), \tag{3}$$

$$\frac{\partial q_j}{\partial x_j} = -\frac{\partial}{\partial x_\perp}\left(\rho\kappa_\perp \frac{\partial T}{\partial x_\perp}\right) - \frac{\partial}{\partial x_\wedge}\left(\rho\kappa_\wedge \frac{\partial T}{\partial x_\wedge}\right) - \frac{\partial}{\partial x_\parallel}\left(\rho\kappa_\parallel \frac{\partial T}{\partial x_\parallel}\right), \tag{4}$$

$$\frac{\partial b_i}{\partial t} = -\epsilon_{ijk}\frac{\partial E_k}{\partial x_j}, \tag{5}$$

$$\frac{\partial b_k}{\partial x_k} = 0, \tag{6}$$

$$E_i = -\epsilon_{ijk}\left(u_j - \frac{\epsilon_H}{\rho} J_j\right) b_k - \frac{\epsilon_H}{\rho}\frac{\partial p_e}{\partial x_i} + \eta J_i, \tag{7}$$

are expressed in the helical-toroidal coordinate system (u^1, u^2, u^3)[3]. The variables ρ, p, u_i, b_i are the mass density, the pressure, the i-th components of the velocity field and the magnetic field vectors, respectively. The symbol Γ denotes the ratio of the specific heats. Plasma is assumed to be an ideal gas: $p = \rho T$ where T is the temperature. The subscripts

$\parallel$, $\perp$, and $\bigwedge$ represents the direction parallel, normal, and binormal to the magnetic field lines, respectively. Equations (1)-(5) are already normalized by representative quantities; the mass density ρ_0, the horizontal width of the vertically-elongated poloidal cross-section $2L_0$, the mean toroidal magnetic field B_0, the vacuum permeability μ_0, the Alfvén velocity $V_A = \sqrt{B_0^2/\mu_0\rho_0}$, and the Alfvén time unit $\tau_A = R_c/V_A$ where R_c is the major radius of the center of the helical coils. The viscous stress tensor Π_{ij} (the viscosity μ is included in it) and the three components of the heat conductivity $\kappa_\perp$, $\kappa_\bigwedge$, and $\kappa_\parallel$ are also normalized by the typical quantities whereas they are given originally in the dimensional form in Braginskii[10] and later in Schnack[11]. In the MINOS code, the spatial derivatives are approximated by the 8th order compact finite difference scheme[12]. The Runge-Kutta-Gill scheme is adopted for the time evolution.

For the purpose of carrying out LESes of the compressible system (1)-(7), the Favre filter is introduced as $\widetilde{u} := \overline{\rho u}/\overline{\rho}$, where $\bar{\cdot}$ indicates a low-pass filter, the cut-off wave number of which is often the same as or comparable to the grid width of a simulation. By the use of the Favre filter and the low-pass filter, the GS components of eqs.(1)-(7) are expressed as

$$\frac{\partial\overline{\rho}}{\partial t} = -\frac{\partial}{\partial x_k}\left(\overline{\rho}\widetilde{u}_k\right), \tag{8}$$

$$\frac{\partial\left(\overline{\rho}\widetilde{u}_k\right)}{\partial t} = -\frac{\partial}{\partial x_j}\left[\left(\overline{\rho}\widetilde{u}_i\widetilde{u}_j - \overline{b}_i\overline{b}_j\right) + \left(\overline{p} + \frac{1}{2}\overline{b}_k\overline{b}_k\right)\delta_{ij}\right] - \frac{\partial}{\partial x_j}\overline{\Pi}_{ij} - \frac{\partial}{\partial x_j}\tau_{ij}, \tag{9}$$

$$\frac{\partial\overline{p}}{\partial t} = -\widetilde{u}_k\frac{\partial\overline{p}}{\partial x_k} - \Gamma\overline{p}\frac{\partial\widetilde{u}_k}{\partial x_k} + (\Gamma-1)\times\left(\eta\overline{J}_k\overline{J}_k + \overline{u}_i\frac{\partial\overline{\Pi}_{ij}}{\partial x_j} - \frac{\partial\widetilde{q}_k}{\partial x_k}\right) - \frac{\partial\Phi_k}{\partial x_k}, \tag{10}$$

$$\frac{\partial\widetilde{q}}{\partial x_j} = -\frac{\partial}{\partial x_\perp}\left(\overline{\rho}\kappa_\perp\frac{\partial\widetilde{T}}{\partial x_\perp}\right) - \frac{\partial}{\partial x_\bigwedge}\left(\overline{\rho}\kappa_\bigwedge\frac{\partial\widetilde{T}}{\partial x_\bigwedge}\right) - \frac{\partial}{\partial x_\parallel}\left(\overline{\rho}\kappa_\parallel\frac{\partial\widetilde{T}}{\partial x_\parallel}\right), \tag{11}$$

$$\frac{\partial\overline{b}_i}{\partial t} = -\epsilon_{ijk}\frac{\partial}{\partial x_j}\left(\overline{E}_k + E_k^M\right), \tag{12}$$

$$\frac{\partial\overline{b}_k}{\partial x_k} = 0, \tag{13}$$

$$\overline{E}_i = -\epsilon_{ijk}\left(\widetilde{u}_j - \frac{\epsilon_H}{\overline{\rho}}\overline{J}_j\right)\overline{b}_k - \frac{1}{\overline{\rho}}\frac{\partial\overline{p}_e}{\partial x_i}. \tag{14}$$

where new variables τ_{ij}, Φ_i, and E_i^M represents the difference of influences of the SGS components on the GS components,

$$\tau_{ij} = \left[\overline{\left(\rho u_i u_j - b_i b_j\right)} + \frac{1}{2}\overline{b_k b_k\delta_{ij}}\right] - \left[\left(\overline{\rho}\widetilde{u}_i\widetilde{u}_j - \overline{b}_i\overline{b}_j\right) + \frac{1}{2}\overline{b}_k\overline{b}_k\delta_{ij}\right], \tag{15}$$

$$\begin{aligned}\frac{\partial\Phi_k}{\partial x_k} = &-\left(\overline{u_k\frac{\partial p}{\partial x_k}} + \overline{\Gamma p\frac{\partial u_k}{\partial x_k}}\right) + \left(\widetilde{u}_k\frac{\partial\overline{p}}{\partial x_k} + \Gamma\overline{p}\frac{\partial\widetilde{u}_k}{\partial x_k}\right)\\ &+(\Gamma-1)\times\left[\eta\left(\overline{J_kJ_k} - \overline{J}_k\overline{J}_k\right) - \left(\frac{\partial\overline{q}_k}{\partial x_k} - \frac{\partial\widetilde{q}_k}{\partial x_k}\right)\right],\end{aligned} \tag{16}$$

$$E_i^M = \left[-\epsilon_{ijk}\overline{\left(u_j - \frac{\epsilon_H}{\rho}J_j\right)b_k} - \overline{\frac{\epsilon_H}{\rho}\frac{\partial p_e}{\partial x_i}}\right] - \left[\left(\widetilde{u}_j - \frac{\epsilon_H}{\rho}\overline{J}_j\right)\overline{b}_k - \frac{1}{\overline{\rho}}\frac{\partial \overline{p}_e}{\partial x_i}.\right] \quad (17)$$

See Garnier et al.[17] for alternative expressions of GS equations for compressible fluids.

Here we introduce SGS models for τ_{ij}, Φ_i and E_i^M based on earlier studies[8, 4, 9] as

$$\tau_{ij} = -\nu_{SGS}\widetilde{S}_{ij}, \quad (18)$$

$$\Phi_i = -\kappa_{SGS}\overline{\rho}\frac{\partial \widetilde{T}}{\partial x_i}, \quad (19)$$

$$E_i^M = -\eta_{SGS}\overline{J}_i. \quad (20)$$

By the use of this quantity, The SGS viscosity, heat conductivity and the resistivity can be expressed as $\nu_{SGS} = C_\nu \mu_{SGS}$, $\kappa_{SGS} = C_\kappa \mu_{SGS}$, and $\eta_{SGS} = C_\eta \mu_{SGS}$, where

$$\mu_{SGS} = \left(C_\nu \frac{1}{2}\overline{S}_{ij}^2 + C_\eta \overline{J}_i^2\right)^{1/2} \Delta^2. \quad (21)$$

Here $\Delta = (\Delta x_1 \Delta x_2 \Delta x_3)^{1/3}$, $\overline{S}_{ij}$ and $\overline{J}_i$ are the mean computational grid width, the rate of strain tensor and the current density in the grid scale, respectively[8, 9]. This type of SGS model, Smagorinsky model, has long been used for LESes of both hydrodynamic and MHD turbulence. While a Smagorinsky-type model is often used for homogeneous turbulence, it has also been applied successfully for anisotropic and inhomogeneous systems including Rayleigh-Taylor instability[13] and RFP plasmas[14]. However, since $\overline{J}_i$ includes the equilibrium component J_i^{equil}, it can contaminate linear growth of unstable modes. In order to avoid the contamination, we modify the model as

$$\mu_{SGS}^a = \left(C_\nu \frac{1}{2}\overline{S}_{ij}^2 + C_\eta \overline{\left(J_i - J_i^{equil}\right)^2}\right)^{1/2} \Delta^2, \quad (22)$$

$$\mu_{SGS}^b = \left(C_\nu \frac{1}{2}\overline{S}_{ij}^2 + C_\eta \overline{J}_i^2\right)^{1/2} \Delta^2 f_D, \quad (23)$$

$$\nu_{SGS}^a = C_\nu \mu_{SGS}^a, \quad (24)$$

$$f_D = \exp\left(-C_D \frac{\mu}{\nu_{SGS}^a}\right). \quad (25)$$

While $\mu_{SGS} = \mu_{SGS}^b$ can be more suitable than $\mu_{SGS} = \mu_{SGS}^a$ in the context of an LES theory, we show in this paper only the results on $\mu_{SGS} = \mu_{SGS}^a$ because of the restriction of pages. Whether we use $\mu_{SGS} = \mu_{SGS}^a$ or $\mu_{SGS} = \mu_{SGS}^b$, the Smagorinsky constants C_ν, C_κ, C_η and an empirical constant C_D are to be determined by calibration to either precise numerical data or experimental data. We also note that applicability of the models has been examined on homogeneous Hall MHD and single-fluid MHD turbulence under a uniform magnetic field[9]. Our current understanding is that the model can be more suitable for two-fluid MHD model including the Hall term than for single-fluid MHD model. This is another, collateral reason why we study two-fluid SGS model than single-fluid SGS model here.

3 Estimation of the SGS viscosity based on better-resolved simulations

Firstly, we estimate how much the SGS terms can contribute to a mild saturation of unstable modes by making use of our earlier numerical data. Time evolution of μ_{SGS} in eq.(21) by the use of numerical data in Ref.[1] is plotted in Fig.1(a), and isosurfaces of μ at a time of nonlinear saturation is shown in Fig.1(b) for $C_\nu = C_\eta = 0.046$ according to Ref.[8] for incompressible channel MHD turbulence. It has been set $\mu = \kappa = \eta = 1 \times 10^{-6}$ and number of grid points $193 \times 193 \times 640$ in the reference simulation in Ref.[1] and $\mu = 5 \times 10^{-4}$, $\kappa = \eta = 1 \times 10^{-6}$ for the same resolution in Ref.[15]. We recall here that growth of unstable mode in the latter computation is mildly saturated and that well-formed magnetic surfaces are recovered autonomously after the saturation. Since the maximum value of the SGS viscosity in Fig.1(a) is larger than $\mu = 5 \times 10^{-4}$, it is expected that the introduction of the SGS viscosity suppress the saturation level of the instability considerably, although it is also considered that a mild saturation of the instability cannot be achieved only by the introduction of the SGS effects because unstable modes can grow linearly before the SGS effects begin to work.

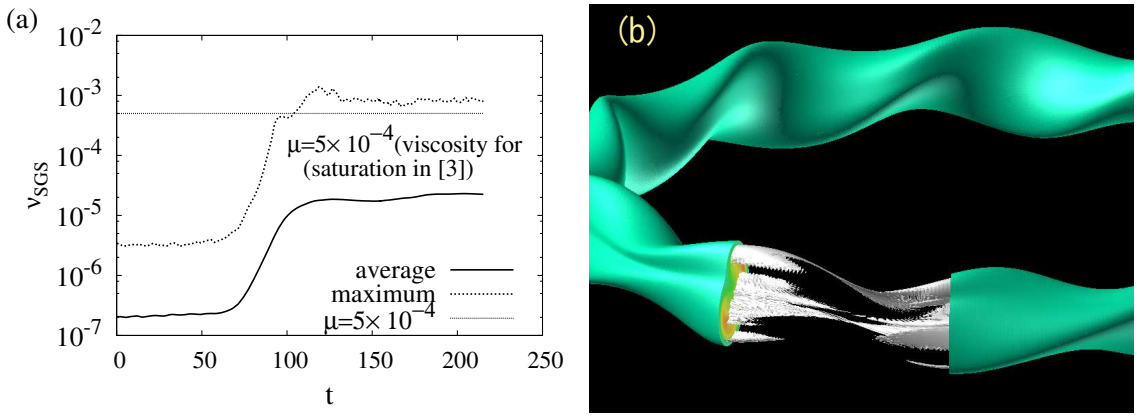

FIG. 1: (a) Time evolution of mean (solid) and the maximum (dotted) values of the SGS viscosity estimated from nonlinear MHD simulation of ballooning modes of LHD. (b) Isosurface of μ defined in eq.(21) in a nonlinear simulation.

Next we carry out LESes of ballooning modes with a smaller number of grid points $97 \times 97 \times 640$ and a coarser time step width. In Fig.2, time evolution of the energy of each toroidal mode n of (a) parallel and (b) normal components of the velocity obtained by an LES of $C_\nu = C_\kappa = C_\eta = 0.046$ is shown. In Fig.2 the power spectra grow exponentially in the beginning of the time evolution, indicating that the linear regime is not contaminated by the introduction of the SGS models. Though the growth rate is the largest in $n = 1$, being contradicting with a nature of ballooning modes, it is the consequence of a large $\kappa_\parallel = 1 \times 10^{-1}$, not of SGS effects. In fact, a simulation with a higher numerical resolution in Ref.[1] also show that the growth rate of the unstable modes is the largest for $n = 1$, in which $\kappa_\parallel = 1 \times 10^{-2}$. It is also noteworthy that the parallel component is quite larger than

the normal component. These results show that our LES reproduces qualitative natures in ballooning modes of LHD with a higher numerical resolution in Ref.[1].

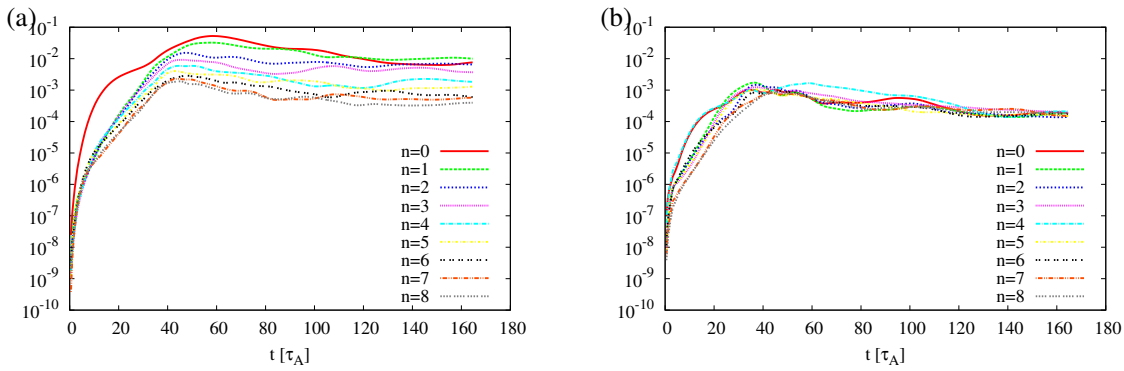

FIG. 2: Time evolution of the energy of each toroidal mode n of (a) parallel and (b) normal components of the velocity obtained by an LES of $C_\nu = C_\kappa = C_\eta = 0.046$.

In Fig.3, the $m = 0$, $n = 0$ component of the pressure is plotted as the function of the initial magnetic flux function $\sqrt{\psi}$. Fig.3(a) is for an LES of (a) $C_\nu = C_\kappa = C_\eta = 0.046$, and Fig.3(b) is for an LES of (b) $C_\nu = C_\kappa = C_\eta = 0.46$. Both of the two runs give a nonlinear saturation even though the numerical resolution is not very fine. Note that a numerical simulation ends in a numerical explosion without the SGS terms for this numerical resolution. Note also that computational cost is about 1/32 or less than the earlier computations reported in Ref.[4] in which the number of grid points is $193 \times 193 \times 640$ and a strong numerical filter is applied to eliminate very fine (both in time and space) motions. While Fig.3(a) gives a more deteriorated profile than that in a two-fluid simulation in Ref.[4] with respect to a saturated P_{00}, the set of the SGS coefficients in (b) gives a better result than both (a) and that in Ref.[4]. These numerical results give an evidence that the LES approach can compensate a lack of numerical resolution in a simulation reasonably and enable a smaller and a quicker numerical simulation, although we have to keep in mind that the SGS coefficients should be calibrated more carefully.

4 Concluding Remarks

In summary, we have developed SGS models suitable for two-fluid/extended MHD equations. Our LESes achieve a nonlinear saturation of ballooning modes by a coarse numerical resolution without contaminating linear growth of unstable modes upto moderate wave number. The LES approach enables a drastic reduction of the computational cost and a better representation of dynamics in two-fluid simulations of strong ballooning modes without damping the modes excessively, and thus provides much easier access to study of saturation mechanism of unstable modes in LHD, although we need calibrations of Smagorinsky constants for very precise numerical computations and experiments (validation). We remark that the existence of the two-fluid term in the induction law of the

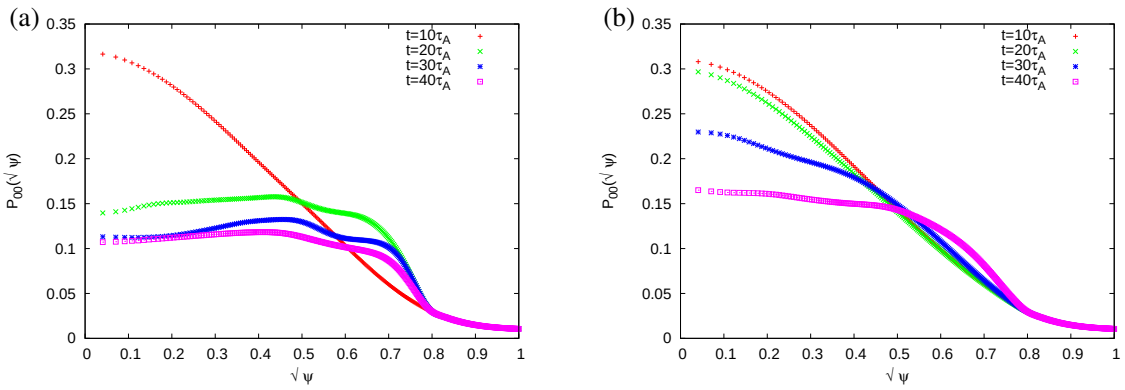

FIG. 3: The mean pressure profile $P_{m=0,n=0}(\sqrt{\psi})$ *in two LESes: (a)* $C_\nu = C_\kappa = C_\eta = 0.046$*, and (b)* $C_\nu = C_\kappa = C_\eta = 0.46$*.*

extended MHD equations can be essential because the two-fluid term is quadratic on the magnetic field, enhancing the forward energy transfer from a large scale to small scale in the wave number space, and enable replacing a part of the sub-grid-scale effects by the Smagorinsky-type models.

This research was partially supported by JSPS KAKENHI Grant Number 23540583 and MEXT KAKENHI Grant Number 15H02218, Japan. This research was also partially supported by the Joint Institute for Fusion Theory (JIFT) program in the US-Japan collaboration for fusion studies. The numerical simulations were performed on the FUJITSU FX100 supercomputer *Plasma Simulator* of NIFS. Some of simulations were performed also on FX100 of Nagoya University based on the HPC project of Nagoya University, and *HELIOS* supercomputer system at Computational Simulation Centre of International Fusion Energy Research Centre (IFERC-CSC), Aomori, Japan.

References

[1] MIURA, H. and NAKAJIMA, N., "Influences of ballooning modes with moderate wave number on MHD equilibrium in LHD", Nucl. Fusion **50** (2010) 054006.

[2] SATO, M. et al., Proc. 22th IAEA-FEC TH/P3-25 (Oct.8-13 2012, San Diego, U.S.A., http://www-naweb.iaea.org/napc/physics/FEC/FEC2012/papers/467_THP325.pdf.

[3] MIURA, H. et al., "Nonlinear Evolution of MHD Instability in LHD", Fusion Sci. Tech. **51** (2007) 8-19.

[4] MIURA, H. et al., "Two-fluid Effects on Pressure-Driven Modes in a Heliotron Device,", the 24th IAEA-FEC TH/P5-17 (Oct. 2014, St. Petersburg, Russia), http://www-naweb.iaea.org/napc/physics/FEC/FEC2014/fec2014-preprints/67_THP517.pdf.

[5] MIURA, H. et al., "Non-disruptive MHD dynamics in inward-shifted LHD configurations", the 20th IAEA-FEC TH/2-3 (Nov. 1-6 2004, Villamoura, Portugal) http://www-pub.iaea.org/MTCD/publications/PDF/CSP-25-CD_front.pdf.

[6] TODO, Y. et al., "Simulation Study of Ballooning Modes in the Large Helical Device", Plasma and Fusion Research **5** (2010) S2062.

[7] GOTO, R. et al., "Formation of large-scale structures with sharp density gradient through Rayleigh-Taylor growth in a two-dimensional slab under the two-fluid and finite Larmor radius effects", Phys. Plasmas **22** (2015) 032115.

[8] HAMBA, F. and TSUCHIYA, M., "Cross-helicity dynamo effect in magnetohydrodynamic turbulent channel flow", Phys. Plasmas 17 (2010) 012301.

[9] MIURA, H., HAMBA, F., and ARAKI, K., "Hall effects and sub-grid-scale modeling in magnetohydrodynamic turbulence simulations", J. Comput. Phys. **316** (2016) 386-395.

[10] BRAGINSKII, S.I. "Transport Processes in a Plasma", in *Reviews of Plasma Physics*, edited by M. A. Leontovich (Consultants Bureau, New York, 1965), volume.1, p. 205.

[11] SCHNACK, D.D. et al., "Computational modeling of fully ionized magnetized plasmas using the fluid approximation", Phys. Plasmas **13** (2006) 058103

[12] LELE, S., "Compact finite difference schemes with spectral-like resolution", J. Comput. Phys. **103** (1992) 16–42.

[13] CABOT, W.H., COOK, A.W., "Reynolds number effects on Rayleigh-Taylor instability with possible implication for type Ia supernova", Nature Physics **2** (2006) 562-568.

[14] HAMBA, F., "Numerical simulation of reversed field pinches using a turbulence model", J. Phys. Soc. Japan **58** (1989) 2414-2422.

[15] MIURA, H. et al., "Direct Numerical Simulation of Nonlinear Evolution of MHD Instability in LHD", Theory of Fusion Plasmas Joint Varenna-Lausanne International Workshop (Varenna, Italy, August 28-September 1, 2006), AIP Conference Proceedings **871** (2006) 157–168.

[16] CHERMYSHOV, A.A., KARELSKY, K.V., and PETROSYAN, A.S., "Subgrid-scale modelling of compressible magnetohydrodynamic turbulence in heat-conduction plasma", Phys. Plasmas **13** (2006) 104501.

[17] GRNIER, E., ADAMS, N., and SAGAUT, P., Large Eddy Simulation for Compressible Flows, Springer (2009).